Fast response in-line gas sensor using C-type fiber and Ge-doped ring defect photonic crystal fiber

Sahar Hosseinzadeh Kassani,[1] Jiyoung Park,[1] Yongmin Jung,[2] Jens Kobelke,[3] and Kyunghwan Oh[1,*]

[1]*Photonic Device Physics Laboratory, Institute of Physics and Applied Physics, Yonsei University, Seoul 120–749, South Korea*

[2]*Optoelectronics Research Centre, University of Southampton, Southampton, UK*

[3] *Institute of Photonic Technology, Jena, Germany*

[*]*koh@yonsei.ac.kr*

Abstract: An in-line chemical gas sensor was proposed and experimentally demonstrated using a new C-type fiber and a Ge-doped ring defect photonic crystal fiber (PCF). The C-type fiber segment served as a compact gas inlet/outlet directly spliced to PCF, which overcame previous limitations in packaging and dynamic responses. C-type fiber was prepared by optimizing drawing process for a silica tube with an open slot. Splicing conditions for SMF/C-type fiber and PCF/C-type fiber were experimentally established to provide an all-fiber sensor unit. To enhance the sensitivity and light coupling efficiency we used a special PCF with Ge-doped ring defect to further enhance the sensitivity and gas flow rate. Sensing capability of the proposed sensor was investigated experimentally by detecting acetylene absorption lines.

OCIS codes: (060.2370) Fiber optics sensors; (060.5295) Photonic crystal fibers; (280.4788) Optical sensing and sensors; (060.2280) Fiber design and fabrication.

References and links

1. J. C. Kim, H. K. Kim, U. C. Paek, B. H. Lee, and J.-B. Eom, "The Fabrication of a Photonic Crystal Fiber and Measurement of its Properties," J. Opt. Soc. Korea **7**(2), 79–83 (2003).
2. T. M. Monro, W. Belardi, K. Furusawa, J. C. Baggett, N. G. R. Broderick, and D. J. Richardson, "Sensing with microstructured optical fibres," Meas. Sci. Technol. **12**(7), 854–858 (2001).
3. V. P. Minkovich, D. Monzón-Hernández, J. Villatoro, and G. Badenes, "Microstructured optical fiber coated with thin films for gas and chemical sensing," Opt. Express **14**(18), 8413–8418 (2006).
4. V. Matejec, J. Mrázek, M. Hayer, I. Kašík, P. Peterka, J. Kaňka, P. Honzátko, and D. Berková, "Microstructure fibers for gas detection," Mater. Sci. Eng. C **26**(2–3), 317–321 (2006).
5. T. M. Monro, D. J. Richardson, and P. J. Bennett, "Developing holey fibres for evanescent field devices," Electron. Lett. **35**(14), 1188–1189 (1999).
6. J. M. Fini, "Microstructure fibres for optical sensing in gases and liquids," Meas. Sci. Technol. **15**(6), 1120–1128 (2004).
7. T. P. Hansen, J. Broeng, C. Jakobsen, G. Vienne, H. R. Simonsen, M. D. Nielsen, P. M. W. Skovgaard, J. R. Folkenberg, and A. Bjarklev, "Air-Guiding Photonic Bandgap Fibers: Spectral Properties, Macrobending Loss, and practical handling," J. Lightwave Technol. **22**(1), 11–15 (2004).
8. I. Dicaire, J. C. Beugnot, and L. Thévenaz, "Analytical modeling of the gas-filling dynamics in photonic crystal fibers," Appl. Opt. **49**(24), 4604–4609 (2010).
9. K. Nielsen, D. Noordegraaf, and T. Sørense, "Selective filling of photonic crystal fibres," J. Opt. A, Pure Appl. Opt. **7**(13), 1464–4258 (2005).
10. T. Ritari, J. Tuominen, H. Ludvigsen, J. Petersen, T. Sørensen, T. Hansen, and H. Simonsen, "Gas sensing using air-guiding photonic bandgap fibers," Opt. Express **12**(17), 4080–4087 (2004).
11. Y. L. Hoo, W. Jin, C. Shi, H. L. Ho, D. N. Wang, and S. C. Ruan, "Design and modeling of a photonic crystal fiber gas sensor," Appl. Opt. **42**(18), 3509–3515 (2003).
12. C. J. Hensley, D. H. Broaddus, C. B. Schaffer, and A. L. Gaeta, "Photonic band-gap fiber gas cell fabricated using femtosecond micromachining," Opt. Express **15**(11), 6690–6695 (2007).

#188272 - $15.00 USD Received 3 Apr 2013; revised 29 May 2013; accepted 31 May 2013; published 5 Jun 2013

13. F. M. Cox, R. Lwin, M. C. J. Large, and C. M. B. Cordeiro, "Opening up optical fibres," Opt. Express **15**(19), 11843–11848 (2007).
14. C. M. B. Cordeiro, M. A. R. Franco, G. Chesini, E. C. S. Barretto, R. Lwin, C. H. Brito Cruz, and M. C. J. Large, "Microstructured-core optical fibre for evanescent sensing applications," Opt. Express **14**(26), 13056–13066 (2006).
15. Z. Zhi-guo, Z. Fang-di, Z. Min, and Y. Pei-da, "Gas sensing properties of index-guided PCF with air-core," Opt. Laser Technol. **40**(1), 167–174 (2008).
16. J. Park, S. Lee, S. Kim, and K. Oh, "Enhancement of chemical sensing capability in a photonic crystal fiber with a hollow high index ring defect at the center," Opt. Express **19**(3), 1921–1929 (2011).
17. L. Xiao, M. S. Demokan, W. Jin, Y. Wang, and C. L. Zhao, "Fusion splicing photonic crystal fibers and conventional single-mode fibers: microhole collapse effect," J. Lightwave Technol. **25**(11), 3563–3574 (2007).
18. K. Saitoh and M. Koshiba, "Full-vectorial imaginary-distance beam propagation method based on a finite element scheme: Application to photonic crystal fibers," J. Quantum Electron. **38**(7), 927–933 (2002).
19. K. T. V. Grattan and B. T. Meggitt, *Optical Fiber Sensor Technology*, **4** (Kluwer Academic, 1999), Chapter 2.
20. W. C. Swann and S. L. Gilbert, "Pressure-induced shift and broadening of 1510–1540-nm acetylene wavelength calibration lines," J. Opt. Soc. Am. B **17**(7), 1263–1270 (2000).
21. S. L. Gilbert, W. C. Swann, *Acetylene $^{12}C_2H_2$ absorption reference for 1510 nm to 1540 nm wavelength* (NIST special publication, 2001).

1. Introduction

In recent years, micro-structured optical fibers, especially photonic crystal fibers (PCFs) [1], have attracted considerable interests for sensing applications due to the fact that micro-holes in PCFs can provide a strong interaction between the guided light with gases or liquids filled there within [2–6]. In terms of the overlap between the light and gas/liquid paths, photonic band gap fiber (PBGF) can provide the highest interaction strength, yet index guiding PCFs have been used as a practical sensing medium due to limited transmission bands of PBGF and better interconnection with conventional single mode fibers (SMFs) [7].

In PCF-based sensor, however, the rate of gas diffusion into the micron-sized holes caused various limitations in sensing capability [8, 9]. Several ideas have been proposed to overcome this issue, which mainly dealt with designing the inlet/outlet components connected to PCFs for efficiently flowing measurands into the holes of fiber. While the butt coupling method is the most general approach [10], other methods such as using periodic openings [11], drilling holes in PCF with a femtosecond laser [12] and drawing fiber with a laterally slotted preform [13] also have been proposed for the gas inlet/outlet. However, those methods still have raised significant difficulties: requirement of elaborated alignment processes for each measurement, broken symmetry in the periodic structure of the PCF, too small holes for efficient measurand entry, as well as sophisticated fabrication processes. Improving the sensing sensitivity in PCF is still an on-going critical issue [14, 15].

In this study, we demonstrated an-all fiber gas sensor unit by proposing a novel 'C-type' fiber as an inlet/outlet component and utilizing a special Ge-doped ring defect PCF to solve prior limitations such as slow flow, broken symmetry in PCF, and tedious alignment. We fabricated the C-type fiber by a well-established glass working technique and fiber drawing procedures at a relatively low temperature around 1850~1900° C using a commercial silica glass tube with an axial slot. The diameter of the C-type fiber was same as that of SMF and PCF, which allows it to be spliced effectively. Moreover, using C-type fiber as a gas inlet/outlet allowed us seamlessly concatenated all-fiber sensor unit for versatile gas detection applications.

The C-type fiber inlet/outlets were directly fusion spliced to the special PCF as well as SMF with an optimal arc condition to maintain the light guidance along different segments of optical fibers. We used a Ge-doped ring defect PCF as a sensing medium which has a higher sensitivity than conventional index-guided PCF with a central silica defect, as it provided a larger overlap between the optical field and the sensing species [16]. We numerically analyzed this special PCF using a full-vectorial finite element method (FEM) comparing its sensitivity with that of a conventional PCF. Acetylene gas was selected as an example for experimentally investigating the performance of the fabricated sensor unit. Characteristic

#188272 - $15.00 USD Received 3 Apr 2013; revised 29 May 2013; accepted 31 May 2013; published 5 Jun 2013

absorption lines were clearly observed as a 25-cm long composite fiber sensor unit was filled with a mixture of acetylene and nitrogen gases at various pressure levels. The dynamic response of the sensor was also quantified in detail.

2. Device design and fabrication

A schematic diagram of the proposed device is shown in Fig. 1(a). The sensor system is composed of a signal light guiding fiber which is single mode fiber (SMF) placed at both ends. The sensing part is PCF with Ge-doped ring defect. The C-type fibers were spliced at both ends of PCF to form the inlet/outlet routes for the gas. We fabricated the C-type fiber by drawing a commercial silica glass tube at a relatively low temperature around 1850~1900° after making a lateral slot in the preform as shown in Fig. 1(b). Figure 1(c) shows the cross sectional image of the fabricated C-type fiber used in this experiment, which has a diameter of 125μm compatible to SMF and PCF. The diameter of hollow hole, d_{hole}, in the central region is 36.5μm with an opening angle θ = 65°. Note that both d_{hole} and θ are sufficiently large to make the C-type fiber a desirable inlet/oulet compatible to conventional optical fibers. The diameter of the C-type fiber was deliberately kept the same as that of SMF and PCF, which allows it to be spliced effectively. In Fig. 1(d), the cross section of the Ge-doped ring defect PCF is shown. Note that there is no central silica defect, yet the light guidance was achieved by the high refractive index Ge-doped ring defect [16], as will be described in the following section.

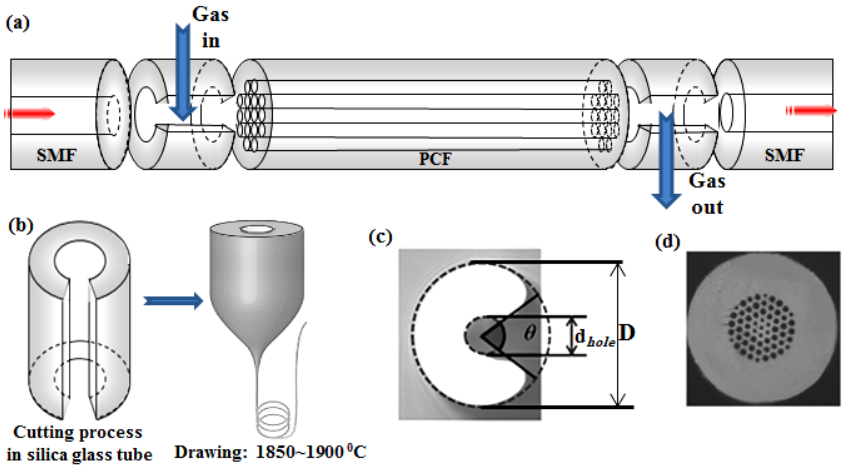

Fig. 1. (a) Schematic diagram of the proposed gas sensor device including single mode fibers (SMF) connected to the light source and the detector, photonic crystal fiber (PCF) as a sensing medium, and C-type fibers as inlet/outlet components. (b) Fabrication process of the C-type fiber. (c) Cross section of the C-type fiber. Material: fused silica, D = 125μm, d_{hole} = 36.5μm and open angle θ = 65°.(d) Cross section of the PCF used in experiment

In the proposed gas sensor unit, two important considerations should be made: 1) optimizing the C-type fiber length, and 2) minimizing the collapse of air holes at the interface between the PCF and C-type fibers. To determine the proper length of C-type fiber, the effect of C-type fiber length over the transmission was compared with the free-space guiding. For a given distance between PCF and SMF, transmission was measured through the C-type fiber and then by-passing it. The results are summarized in Fig. 2. We found that a longer C-type fiber induced more loss in a logarithmic scale, which could be attributed to expansion of the light beam diameter and its reflection and/or scattering at the inner surface of the C-type fiber. Therefore, we chose the length of the C-type fiber less than 60μm in the experiments.

#188272 - $15.00 USD Received 3 Apr 2013; revised 29 May 2013; accepted 31 May 2013; published 5 Jun 2013

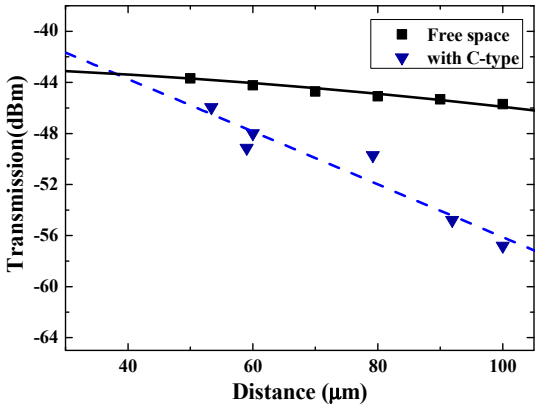

Fig. 2. Effect of C-type length on optical transmission compared with the free space guiding.

We used a fusion splicer (Ericsson FSU975) and an ultra-sonic cleaver (DC-125) to assemble the composite fiber optic sensor unit. As shown in Fig. 3, C-type fiber was spliced to the single mode fiber (SMF-28) and two ends of PCF were spliced to the C-type fiber. Since PCF and C-type fiber structures and melting status are different from the conventional SMF, optimal splicing parameters were investigated to obtain a low-loss joint with a good mechanical strength, which are summarized in Table 1.

Fig. 3. Fabrication of the composite sensor unit by using a single mode fiber (SMF) spliced to the C-type fiber (CF) and then spliced to the photonic crystal fiber (PCF) on one side.

Table1. Optimized parameters of splicing different fibers

Fiber types	Pre-fusion		Fusion1		Fusion2		Fusion3		Center (μm)	Overlap (μm)
	Time (s)	Current (mA)	Time (s)	Current (mA)	Time (s)	Current (mA)	Time (s)	Current (mA)		
SMF/SMF	0.2	10	0.3	10.5	2	16.3	2	12.5	255	10
SMF/C-type	0.2	5	0.1	3	2	11	1	4	245	4
C-type/PCF	0.2	5	0	0	1	9	0	0	205	3

Due to the air–silica structure of PCF and C-type fiber, the softening point of these fibers was significantly lower than that of the solid SMF. To avoid the air hole collapses in the vicinity of the C-type/PCF splice joint, we used a lower fusion current and a shorter fusion time compared to the SMF/SMF splicing condition. We also applied a less amount of heat to the PCF and C-type joint by offsetting the arc position from the center. We set the arc offset from the center, 245 and 205 μm in the case of SMF/C and C/PCF splices, which correspond to an offset distance of 10 μm and 50 μm respectively. We also optimized the overlap which is the distance over which the PCF and C-type fiber are pushed together, which affects the

#188272 - $15.00 USD Received 3 Apr 2013; revised 29 May 2013; accepted 31 May 2013; published 5 Jun 2013

center alignment and subsequently the coupling loss [16]. We fabricated the sensing unit composed of Ge-doped ring defect PCF of 25-cm long whose ends were spliced to C-type fiber segment of ~60μm long. The C-type was fusion spliced to SMF which serves as the light signal input and output.

The photonic crystal fiber utilized in this experiment has GeO_2-doped hollow ring defects to raise the local refractive index at the center. The schematic structures of the the conventional PCF with the silica central defect and the special PCF are shown in Fig. 4(a), and (b) respectively. Note that the special PCF does not have central solid defect provides additional central hole where the light can interact with the gas directly, which will increase the sensitivity [16]. We numerically analyzed this PCF structure using a full-vectorial finite element method (FEM) [18]. The sensitivity f, is the ratio of the optical power over the sample area (the holes in PCFs) to the total cross section of the incident beam [19],

$$f = \int_{sample} \mathrm{Re}(E_x H_y^* - E_y H_x^*) \Big/ \int_{total} \mathrm{Re}(E_x H_y^* - E_y H_x^*)\, dxdy \qquad (1)$$

where $E_{x,y}$ and $H_{x,y}$ are the transverse electric and magnetic field components of the guided fundamental mode. The sensitivity was estimated in the spectral range from 1400 to 1650nm and the results are shown in Fig. 4(c). At λ = 1530.3 nm, the P9 absorption line of acetylene gas, the sensitivity of our PCF was about 4-times higher than that of a conventional PCF.

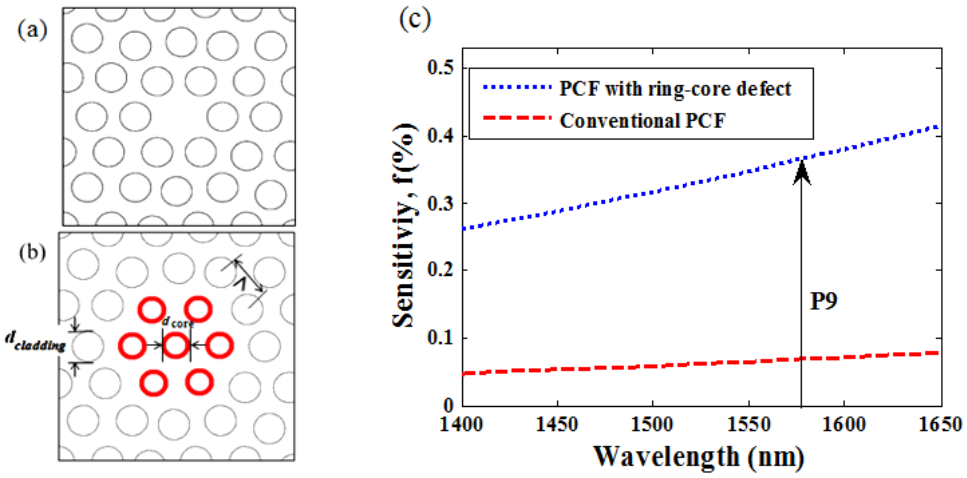

Fig. 4. (a) Conventional PCF, (b) proposed PCF with a hollow high index ring defect, (c) sensitivity calculation of proposed PCF. The core holes and cladding holes are d_{core} = 3.4 μm, and $d_{cladding}$ = 4.6 μm, respectively. The ratio of $d_{cladding}/\Lambda$ and d_{core}/Λ are 0.64 and 0.52, where Λ is pitch size.

3. Experimental results and discussions

To experimentally examine the sensing capability of this device, acetylene gas (C_2H_2) was chosen as a standard measurand. The schematic of the experimental set up is shown in Fig. 5. Light from an Er-doped amplified spontaneous emission (ASE) source passed through the fiber optic sensing unit and measurements were done using an optical spectrum analyzer (OSA) and a power meter. A tunable optical filter (TOF) was also used to control the ASE bandwidth.

#188272 - $15.00 USD Received 3 Apr 2013; revised 29 May 2013; accepted 31 May 2013; published 5 Jun 2013

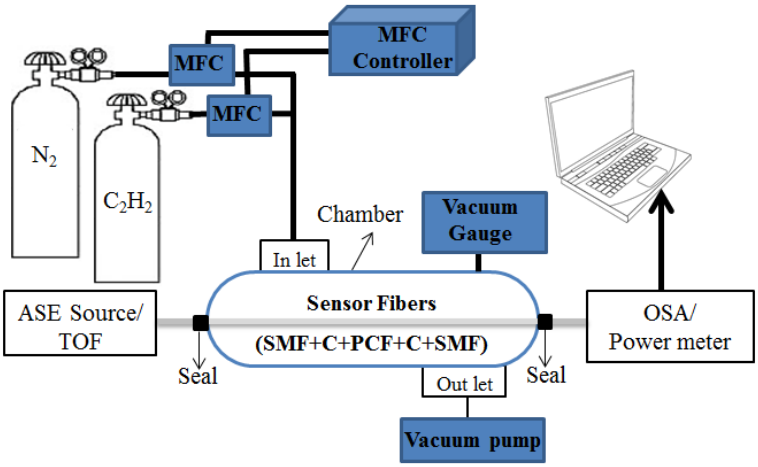

Fig. 5. Experimental set up for investigating sensing capability of the proposed fiber optic sensor unit. A tunable optical filter (TOF) was used to narrow the light bandwidth before coupling light into the fiber. The transmission spectrum was monitored using an optical spectrum analyzer (OSA)

The gas chamber containing the fiber optic sensor unit was evacuated to 10^{-2} Torr by a vacuum pump at room temperature. Then the chamber was filled with a mixture of acetylene (C_2H_2) and nitrogen (N_2) gases. Using high accuracy mass flow controllers (MFC), we could vary the partial pressure of acetylene and nitrogen gases. The total pressure inside the chamber was monitored by a vacuum gauge. When the pressure reached 1 atm (~760 Torr), the chamber pressure was maintained during the experiments to eliminate pressure effects in the sensing mechanism [20].

For a mixture of acetylene and nitrogen gases at a flow rate of 20 sccm, we tried to locate the absorption bands utilizing broadband C-band ASE source (FiberLabs, AMP-FL 8013-CB). The transmission spectra were measured using an optical spectrum analyzer (OSA, Hewlett Packard, 86142A). As acetylene gas was injected to the chamber, its characteristic absorption lines were observed as summarized in Fig. 6. Here the chamber pressure was 400 Torr. The background spectrum and the spectrum in the presence of acetylene gas in Fig. 6 were normalized to give effective transmission spectra as shown in Fig. 7. Acetylene gas has rotational-vibrational absorption bands in the 1510~1545 nm range and we could identify P9, P10 and P11 lines distinctively, whose spectral positions are known to be at 1530.3714 nm, 1530.9766 nm and 1531.5882 nm, respectively in the reference data [21].

#188272 - $15.00 USD Received 3 Apr 2013; revised 29 May 2013; accepted 31 May 2013; published 5 Jun 2013

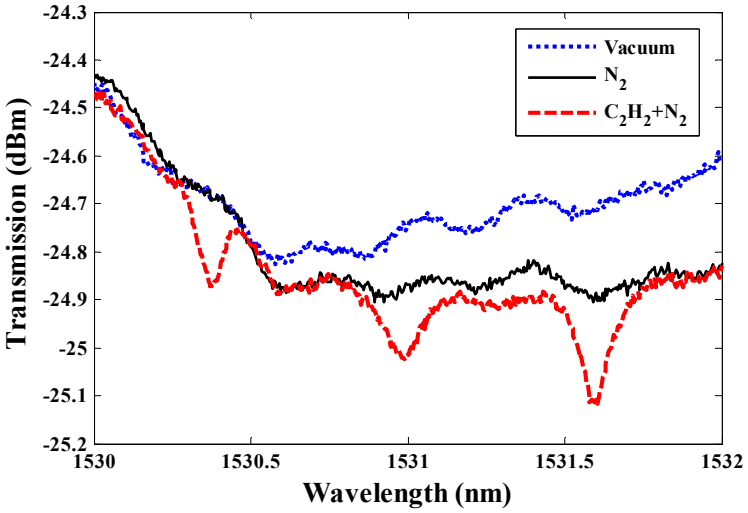

Fig. 6. Optical transmission through the fabricated gas sensor. Background spectrum and spectrum in presence of acetylene gas in the 25-cm long PCF.

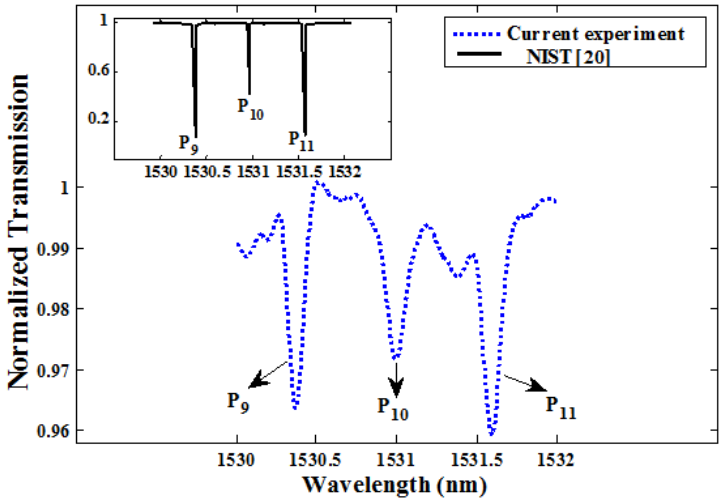

Fig. 7. P9, P10 and P11 absorption lines for mixture of acetylene and nitrogen gases

Figure 8 shows the transmission change near P9 line as the concentration of the acetylene gas varied to 0.5, 2.5, and 4.07%, at the total pressure of 1 atm.

#188272 - $15.00 USD Received 3 Apr 2013; revised 29 May 2013; accepted 31 May 2013; published 5 Jun 2013

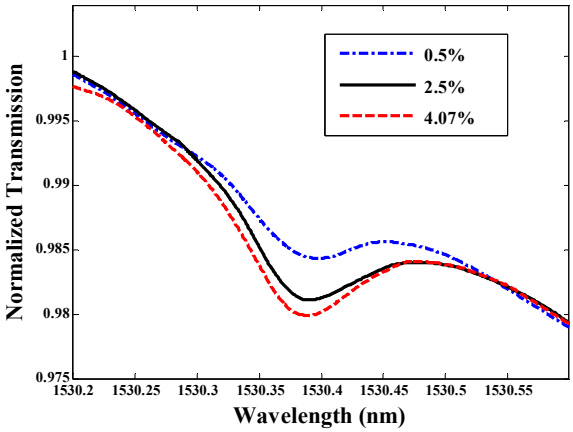

Fig. 8. Transmission near the P9 absorption line for different concentrations of the acetylene gas while keeping the total pressure at 1 atm.

After identifying the P9 absorption line, we further investigated the dynamic response of the fabricated sensor unit. We used a tunable optical filter (TOF) to select only the light signal near P9 absorption line at 1530.3714 nm. Its transmission power variation by acetylene absorption within the sensor unit was measured using a power meter in real time. Figure 9(a) shows the dynamic response of the sensor unit for various acetylene concentrations in the gas mixture. In order to investigate the dynamic response, firstly the chamber was evacuated to the vacuum level about 10^{-2} Torr, then a specific amount of acetylene and nitrogen gases were released into the chamber. When the partial pressure of the chamber reached 400 Torr, gas injection was stopped for the light signal power measurements, and then the chamber was evacuated again. These steps were repeated with varying the amount of acetylene gases to 4.84%, 3.23%, 1.61% and 0.53% while keeping the total pressure at 400 Torr. As shown in Fig. 9(a), at a higher acetylene gas concentration of 4.84%, the transmission dropped to a saturated level within 14.8 minute. At a lower concentration of 0.53%, it took about ~28 min to reach the signal saturation. Note that the response time did not scale with the concentration such that even the concentration decreased by ~1/9 (from 4.84% to 0.53%), the response time increased only by factor of 1.9 (14.8 to 28.3 minute).

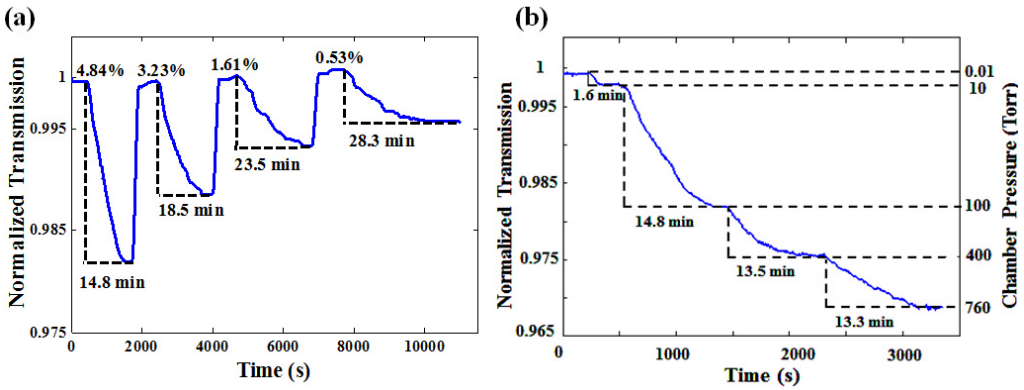

Fig. 9. (a) Dynamic response of the fabricated sensor device for different concentrations of the acetylene gas while keeping the total pressure at 1 atm with adding nitrogen gas (b) Dynamic response of the fabricated sensor in different pressures; gas injection to the chamber stopped at 10, 100, 400 and 760 Torr.

#188272 - $15.00 USD Received 3 Apr 2013; revised 29 May 2013; accepted 31 May 2013; published 5 Jun 2013

Compared with a prior reports based on conventional PCF with a single opening gap inlet of 50μm between butt-coupled PCF and SMF, the filling process for a 25 cm-long PCF took ~8000 s (133 min) at the atmospheric pressure [11]. Our proposed fiber optic sensor unit, with the same length of PCF, the same gas type and the same pressure showed at least ~4 times faster dynamic response even at a low concentration of ~0.5%. This improvement in response time is mainly attributed to our unique C-type fiber inlet/outlet which allows faster gas flow into the PCF.

The sensor's sensitivity was mainly improved by the special PCF structure. As we showed in Fig. 4(c), the Ge-doped ring defect PCF can improve the sensitivity about 4-times higher than that of a conventional PCF. On the other hand, the role of C-type fiber was to provide more gas into the holes to interact with light in a shorter time to improve temporal response. Our comparisons indicated the special PCF and C-type fiber inlet/outlet contributed to a higher sensitivity and a faster dynamic response of the proposed sensor unit, respectively.

The dynamic response of the fabricated sensor at various pressures was also examined and the results are summarized in Fig. 9(b). The chamber was initially evacuated to 10^{-2} Torr then filled with acetylene gas at a flow rate of 20 sccm. When the partial pressure of the chamber reached 10 Torr, gas injection was stopped and the saturated transmitted power was measured. Then the gas injection was continued until pressure reached to 100, 400, and finally 760 Torr. We could observe clear steps in the transmission irrespective of the pressure. Even at a relatively low total pressure of ~10 Torr, the sensor could successfully identify the measurand. Note that this sensing capability of the device at a low pressure can provide a high potential in in situ real time applications. The transmission drop took 14.8 min until it saturated when the pressure was increased to 100 Torr. As the pressure was increased further, the gas filling took a shorter time such that at a higher pressure of 760 Torr it took about ~13.3 min to reach the signal saturation. Note that these results are also several folds faster than prior reports in terms of the dynamic response.

The sensing capability could be further improved by optimizing the length of PCF and the PCF structure. The schematic structure of the proposed PCF is shown in Fig. 10, the proposed defect provides two additional waveguide parameters as indicated in Fig. 10(b): the thickness w_{ring} and relative index difference Δ_{ring}, of doped ring, which can endow a new degree of freedom in waveguide design for sensor applications.

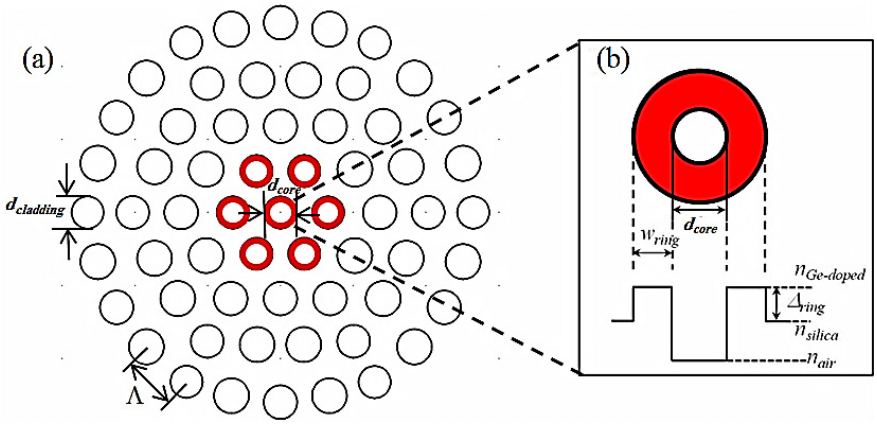

Fig. 10. (a) Proposed PCF with a hollow high index ring defect, (b) its enlarged view with structural parameters: core hole diameter dc, ring width wring, and the relative index difference of the ring Δ ring. The cladding air holes are characterized by their diameter, dcladding, and pitch, Λ .

In our previous work [16], we analysed a new index-guided PCF for chemical sensing applications with a hollow GeO-doped high index ring defect to simultaneously achieve a

#188272 - $15.00 USD Received 3 Apr 2013; revised 29 May 2013; accepted 31 May 2013; published 5 Jun 2013

higher evanescent wave interaction efficiency, a lower confinement loss, and a lower splicing loss than prior PCFs. If we increase the hole size of Ge-doped ring defect, the sensitivity could be further improved due to the increase of the evanescent field overlap with the central hole. The sensitivity can be even more enhanced if we increase the ring width w_{ring} and the relative index difference of the ring Δ_{ring} by providing a tighter confinement of the optical field with a larger overlap with the gas.

Previous papers monitored the dynamic response of hollow fiber-based gas sensors and studied its dependence on fiber length [10,11]. Increasing the fiber length will prolong the sensor response time though it could improve the sensitivity. Therefore, there exists a trade-off between the response time and the sensor sensitivity. The optimum length depends on the molecular species to be monitored and the amount of gas present in the environment. For gases with weak absorption lines or in low concentration, sensitivity enhancement can be obtained by using a longer fiber length.

5. Conclusion

We fabricated an in-line chemical sensing device using novel C-type fiber and Ge-doped ring defect photonic crystal fiber. We demonstrated the all fiber sensor unit which uses 'C-type' fiber as inlet/outlet components can effectively provide a faster gas flux, without distorting PCF structure in seamlessly connected manner. We experimentally found the optimal splicing parameters to avoid air hole collapses in the vicinity of the C-type/PCF splice joint, and to have a properly melted and strong splice joint of SMF/C-type. Using a Ge-doped ring defect photonic crystal fiber we could predict 4-times higher sensitivity than that of a conventional PCF. The sensing efficiency of the proposed device was experimentally investigated using acetylene gas that was flown through a 25-cm length of the Ge-doped ring defect PCF. The P9 line of acetylene was distinctively identified using the proposed device and its dynamic response was also examined. The sensor unit showed more than four times faster dynamics response, which is attributed to C-type fiber in/oulets and the hollow center PCF. We also confirm the sensing capability of the proposed device at a low pressure of 10 Torr. We can further combine C-type fiber in/outlets in other type of holey fibers such as photonic band-gap PCF, hollow optical fiber to further improve sensing capability and dynamic response in all-fiber platform. This device also has high potential to detect biological agents in a liquid along with PDMS micro-fluidic chips, which is being investigated by the authors.

Acknowledgments

This work was supported in part by the National Research Foundation of Korea (NRF) and grant funded by the Korea government (MEST) (No. 2011-00181613), in part by the Seoul R&BD Program (No. PA110081M0212351), in part by the ITEP (10037371-2011-02).

#188272 - $15.00 USD Received 3 Apr 2013; revised 29 May 2013; accepted 31 May 2013; published 5 Jun 2013